Degradable Drug Carriers:

Vanishing Mesoporous Silica Nanoparticles

Karin Möller and Thomas Bein

Department of Chemistry and Center for NanoScience, University of Munich (LMU), Butenandtstrasse 5–13, 81377 Munich, Germany

Fax: (+49) 89-2180-77622

Emails: bein@lmu.de, K.Moeller@lmu.de

Supporting Information

Contents:

Table S-1: Comparing literature results on the dissolution of mesoporous silica and hybrid material

Reference	Form of silica, synthesis conditions	Particle Size	Surf area (m^2/g)/ pore size (nm)	Template removal	Silica Conc. (mg/mL)	Degradation medium	Degradation conditions, analytical method	% dissolution/ time	Conclusions
Porous silicas									
Finnie et al 2009[1]	Porous sol-gel silicas Acidic to neutral	Micron sized: 100, 54, 1.3 µm	373/3 264/13 135/3	na	a) 200 b) 0.04	PBS (+FBS)	37°C a) open flow, 2 mL/min b) Closed system ICP	b) 96, 88, 67%/ 36 h	particles with highest Q^4 dissolved more slowly in open or closed system; FBS slows down dissolution
Choi et al. 2015[2]	SBA-15 acidic; Also grafted w. COOH and NH_2	Micron sized: Ca. 32 µm	1165/7.4	HCl extr. 5h	0.1 (Also 0.5 and 1)	SBF	37°C 150 rpm; ICP	91%/24h COOH: 70%/90h	best degraded with low concentration; functionalized: COOH slowest
He et al. 2010[3]	MSN Basic to neutral	>> 200 nm	a) 958 b) 282/ na	HCl extr. 6h, several times dried; calcined	0.1; (Also 0.3 and 0.5)	SBF	37°C 150 rpm; ICP	a) 90%/ 3h b) 32%/24 h-15d	best degraded with: low concentration, uncalcined, high surface area highly ordered MSNs
Cauda et al. 2010[4]	MSN basic unfunct. or co-cond. w. Cl, NH_2, Ph; + PEG	50-70 nm	1240-632/ 3.2 -3.9	NH_4NO_3 extr. 2x 45 min.	2	SBF	37°C 500 rpm BET	Loss of BET area: 40-60%, pore volume 50-80%, 5 d; Ph: 100% 2h	structural loss: co-cond. with Ph fastest, unfunct. is stable in water PEG slows degradation
Yamada et al. 2012[5]	MSN basic	20, 30, 40, 80 nm	960/4.3	5 X dialysis	Na	PBS	Dialysis Static ICP	90%/ 6d	best degraded when not aggregated, size has no influence
Braun et al. 2016[6]	MSN basic at rt unfunct. or co-cond.	80, 200 1500 nm	760 1200 790 3-4	calcined	0.1	SLF, SBF, SGF	37°C; ICP	80-90%/ 6h	fast dissolution at neutral pH, none in acidic medium, size has no influence
Shen et al. 2014[7]	3D MSN neutral at oil/water interface	100 nm	Ca. 600/ a) 5.5 b) 10	NH_4NO_3 extr.	Na	SBF	TEM	nearly complete in a) 96 h b) 24 h	larger pores degrade fastest
Choi et al. 2017[8]	a) MSN b) MSN+DOX basic	170 nm	a)1328 b) 586/2.4	HCl extr.	1	PBS	37°C static; ICP	Max: a) 61%/8 d b) 72%/8 d	higher dissolution with DOX
Lin et al. 2011[9]	a) MSN b) MSN- basic PEG/TMS	60 nm	a) 1163/2.4 b)629/1.6	HCl extr.	1	SBF	37°C Molybdenum blue test for silica	a) 60 ppm/1-70h b) 60 ppm after 50-70 h	PEG retards dissolution b) TEM after 10 d in SBF nearly unchanged
Hao et al. 2012[10]	MSN basic grafted w. NH_2-PEG	80 nm, also rods 200 and 400 nm	913/2.5	calcined	2	DEMEM or DMEM + 10 % FBS	37°C 150 rpm washed + weighed	50%/60 d	spherical particles degrade faster than rods
Von Haartmann 2016[11]	MSN 10% NH_2 co-condensed + PEI basic	200-300 nm	1100/3.5	HCl extr. 5h	0.12	HEPES	dialysis under shaking 37°C molybdenum blue test for silica	20-25 %/7 d	initially fastest with grafted PEI shell; no influence of hydrophobic cargo

Table S-1 continued: Comparing literature results on the dissolution of mesoporous silica and hybrid materials

Reference	Form of silica, synthesis conditions	Particle Size	Surf area (m^2/g)/ pore size (nm)	Template removal	Silica Conc. (mg/mL)	Degradation medium	Degradation conditions, analytical method	% dissolution/ time	Conclusions
Doped MSNs									
Hao et al. 2015[12]	a) MSN b) Hydroxy-apatite MSN basic	80-90 nm	a) 1546/2 b) 542/15.8	a) HCl extr. 10h b) calcined	2	pH 5	37 °C TEM	a) no change after 12h b) large debris after 4h, 12h: 20 nm residues	b) Ca_2^+ leaching improves dissolution
Pohaku Mitchel et al. 2012[13]	Fe-doped hollow MSN neutral	200 nm	na	calcined	1	Human serum FBS	37°C EDX, SEM	20-25 d	higher dissolution of doped vs. undoped MSN
Yu et al. 2016[14] Wang et al. 2017[15]	a) Mn-doped (180°C 12h) hollow MSN With PEG neutral b) Fe-doped hollow MSN c) MSN	60-70 nm 112	222/3.8	NaCl /MeOH extr. 5h	0.1 500 ppm in 20 mL	SBF without or with GSH without or with deferipro ne	37°C 250 rpm; ICP, TEM 37°C ICP	a) 20 %/36% 2.5 d b) Fe-MSN: 19%/32%/7 d c) MSN: 8%/7 d	Faster degradation of doped MSNs; show in-cell degradation
Hybrid mesoporous silicas*									
Urata et al. 2011[16]	a) Ethylene-bridged MONs, b) MSN basic	20 nm 20 nm	640/7-10	dialysis	Na	PBS	37 °C dialysis ICP	a) 2 % b) 90 % /10 d	pure MSNs degrade much faster than organic-bridged MONs
Croissant et al. 2014[17]	S-S-PMO basic	200 nm spheres 450 nm rods	1059 to 890 /ca. 3	NH_4NO_3 extr.	3	PBS + mercap-to-ethanol	37 °C stirred TEM DLS	partial degradation after 48 h	longer particles degrade faster
Yang et al. 2015[18]	Benzene MON	50 nm	466/ 4.6 941/ 7.6	HCl extr. 6 h	1	DMEM	Dialysis ICP	1 and 2 % silica dissolved after 6 d	
Croissant et al. 2016[19]	Oxamide-phenylene MON basic	100	850/ 2.1	NH_4NO_3 extr.	1.3	PBS + trypsin	37°C stirred TEM weight	2 d: 20 nm fragments 3 d: 68 %	
Yang et al. 2016[20]	S4-MSN TEOS : S-S-silane 1:0.8 neutral	200 nm	405/14 and na/4.6	HCl extr. 6 h	1.5	10 % FBS + GSH	37 °C stirred TEM Ellman	Large morphology change after 48 h	large pore size degrade better in cells; higher degradation in cancer cells
Maggini et al. 2016[21] Prasetyanto et al. 2016[22]	S-S-MSN basic TEOS : S-S-silane 7:3 protein loaded S-S-silica capsules	100 nm 40-50 nm	161/2.2	HCl extr.	0.1	PBS+ DTT, GSH	37°C stirred TEM, UV-VIS of oxidized DTT	particle disintegration after 7d	release of cargo upon S-S reduction
Zhang et al. 2017[23]	S-S- silica NP S-S + DOX silica NP	100 nm	na	na	0.3	PBS + DTT	37 °C In vitro: TEM In vivo: ICP urine	changed morphology after 4 d	DOX incorporation changes dissolution
Huang et al. 2017[24]	S-S-HMONs neutral	40 nm	na/4	HCl extr. 12h	0.1	SBF + GSH	37 °C 300 rpm TEM	after 14 d only debris	stable without GSH for 14 d; *In vitro* and in cell degradation similar
Yu et al. 2018[25]	MSN S-S-MONs neutral	20, 25, 30, 40 nm	around 480/1.8 to 3.8	NaCl in methanol, rt	0.1	SBF + GSH	37 °C 250 rpm TEM, Bio-TEM, ICP, NMR	45 % with or without GSH after 7 d, 80% after 14 d (GSH)	DOX release upon degradation
Datz et al. 2017[26]	Curcumin-MSN basic	200 nm	1040/ 2.8	NH_4NO_3 extr.	2	SBF	37 °C 300 rpm BET, XRD, IR	Stable > 28 d	no degradation experienced

MSN: mesoporous silica nanoparticle, MON: mesoporous organosilica nanoparticle, HMON: hollow mesoporous organosilica nanoparticle, PMO: periodic mesoporous organosilica; na: not available. TMS: trimethyl-chlorosilane; DTT: dithiothreitol; GSH: glutathione; DOX: doxorubicin

*For a recent review on disulfide-bridged organosilicas see Du et al.[27]

[1] K. S. Finnie, D. J. Waller, F. L. Perret, A. M. Krause-Heuer, H. Q. Lin, J. V. Hanna, C. J. Barbé, *J. Sol-Gel Sci. Technol.* **2009**, *49*, 12-18.
[2] Y. Choi, J. E. Lee, J. H. Lee, J. H. Jeong, J. Kim, *Langmuir* **2015**, *31*, 6457-6462.
[3] Q. He, J. Shi, M. Zhu, Y. Chen, F. Chen, *Micropor. Mesopor. Mater.* **2010**, *131*, 314-320.
[4] a) V. Cauda, A. Schlossbauer, T. Bein, *Micropor. Mesopor. Mater.* **2010**, *132*, 60-71; b) V. Cauda, C. Argyo, T. Bein, *J.Mater. Chem.* **2010**, *20*, 8693-8699.
[5] H. Yamada, C. Urata, Y. Aoyama, S. Osada, Y. Yamauchi, K. Kuroda, *Chem. Mater.* **2012**, *24*, 1462-1471.
[6] K. Braun, A. Pochert, M. Beck, R. Fiedler, J. Gruber, M. Linden, *J. Sol-Gel Sci. Technol.* **2016**, *79*, 319-327.
[7] D. Shen, J. Yang, X. Li, L. Zhou, R. Zhang, W. Li, L. Chen, R. Wang, F. Zhang, D. Zhao, *Nano Letters* **2014**, *14*, 923-932.
[8] E. Choi, S. Kim, *Langmuir* **2017**, *33*, 4974-4980.
[9] Y.-S. Lin, N. Abadeer, K. R. Hurley, C. L. Haynes, *J. Am. Chem. Soc.* **2011**, *133*, 20444-20457.
[10] N. Hao, H. Liu, L. li, D. Chen, L. Li, F. Tang, *In Vitro Degradation Behavior of Silica Nanoparticles Under Physiological Conditions, J. Nanosci. Nanotech.* **2012**, 12, 6346-6354.
[11] E. von Haartman, D. Lindberg, N. Prabhakar, J. M. Rosenholm, *Eur. J. Pharm. Sci.* **2016**, *95*, 17-27.
[12] X. Hao, X. Hu, C. Zhang, S. Chen, Z. Li, X. Yang, H. Liu, G. Jia, D. Liu, K. Ge, X.-J. Liang, J. Zhang, *ACS Nano* **2015**, *9*, 9614-9625.
[13] K. K. Pohaku Mitchell, A. Liberman, A. C. Kummel, W. C. Trogler, *J. Am. Chem. Soc.* **2012**, *134*, 13997-14003.
[14] L. Yu, Y. Chen, M. Wu, X. Cai, H. Yao, L. Zhang, H. Chen, J. Shi, *J. Am. Chem. Soc.* **2016**, *138*, 9881-9894.
[15] L. Wang, M. Huo, Y. Chen, J. Shi, *Adv. Healthcare Mater.* **2017**, 1700720-n/a.
[16] C. Urata, H. Yamada, R. Wakabayashi, Y. Aoyama, S. Hirosawa, S. Arai, S. Takeoka, Y. Yamauchi, K. Kuroda, *J. Chem. Soc.* **2011**, *133*, 8102-8105.
[17] J. Croissant, X. Cattoen, M. W. C. Man, A. Gallud, L. Raehm, P. Trens, M. Maynadier, J.-O. Durand, *Adv. Mater.* **2014**, *26*, 6174-6180.
[18] Y. Yang, Y. Niu, J. Zhang, A. K. Meka, H. Zhang, C. Xu, C. X. C. Lin, M. Yu, C. Yu, *Small* **2015**, *11*, 2743-2749.
[19] J. G. Croissant, Y. Fatieiev, K. Julfakyan, J. Lu, A.-H. Emwas, D. H. Anjum, H. Omar, F. Tamanoi, J. I. Zink, N. M. Khashab, *Chem.– Eur. J.* **2016**, *22*, 14806-14811.
[20] Y. Yang, J. Wan, Y. Niu, Z. Gu, J. Zhang, M. Yu, C. Yu, *Chem. Mater.* **2016**, 28, (24), 9008-901
[21] L. Maggini, I. Cabrera, A. Ruiz-Carretero, E. A. Prasetyanto, E. Robinet, L. De Cola, *Nanoscale* **2016**, *8*, 7240-7247.
[22] E. A. Prasetyanto, A. Bertucci, D. Septiadi, R. Corradini, P. Castro-Hartmann, L. De Cola, *Angew. Chem., Int. Ed.* **2016**, *55*, 3236.
[23] Q. Zhang, C. Shen, N. Zhao, F.-J. Xu, *Adv. Funct. Mater.* **2017**, *27*.
[24] P. Huang, Y. Chen, H. Lin, L. Yu, L. Zhang, L. Wang, Y. Zhu, J. Shi, *Biomaterials* **2017**, *125*, 23-37.
[25] L. Yu, Y. Chen, H. Lin, W. Du, H. Chen, J. Shi, *Biomaterials* **2018**, *161*, 292-305.
[26] S. Datz, H. Engelke, C. v. Schirnding, L. Nguyen, T. Bein, *Micropor. Mesopor. Mater.* **2016**, *225*, 371-377.
[27] X. Du, F. Kleitz, X. Li, H. Huang, X. Zhang, S.-Z. Qiao, *Adv. Funct. Mater.* **2018**, *28*, 1707325.
[28] F. Gao, P. Botella, A. Corma, J. Blesa, L. Dong, *J. Phys. Chem. B* **2009**, *113*, 1796-1804.
[29] K. Möller, K. Müller, H. Engelke, C. Bräuchle, E. Wagner, T. Bein, *Nanoscale* **2016**, *8*, 4007-4019.

Experimental Section

Materials

All chemicals were used as received. Ammonium fluoride (NH_4F, Fluka) , 1,3,5-Triisopropylbenzene (TiPB; Fluka), Cetyltrimethylammonium chloride, 25% solution in water (CTAC, Sigma-Aldrich), Triethanolamine (TEA; Fluka), Tetraethoxysilane (TEOS), 3-Aminopropyltriethoxysilane (APTES), (3-Mercaptopropyl)triethoxysilane > 80% (MTES), Phenyltriethoxysilane (PhTES), bisilane bis(3-triethoxysilylpropyl)disulfide (BTDS) and bi-silane bis(3-triethoxysilylpropyl)tetrasulfide (BTES; both > 90%, both Sigma-Aldrich), Pluronic F-127 (Sigma-Aldrich), 1,2,4-Trimethylbenzene (TMB; Sigma-Aldrich), Methoxypolyethylene glycol maleimide MW 750 (PEG; Iris Biotech)), EZ-Link HPDP-Biotin (ThermoFisher), Avidin from egg white (Sigma-Aldrich), 1,2-dioleoyl-3-trimethylammonium-propane (chloride salt) (DOTAP; Avanti), DL-Dithiothreitol (DTT), L-Glutathione reduced (GSH), ATTO-633 maleimide and ATTO-488 NHS ester (both ATTO-Tech),

MSN synthesis at basic pH:
Time-delayed co-condensation synthesis

Medium-sized (about 120 nm) MSN-synthesis with co-condensation of 9 mol% amino-groups in core and 1 mol% mercapto-groups in shell (sample M-C):
Solution 1: 100 mg NH_4F (2.7 mmol), 21.7 mL H_2O (1.12 mol), 2.97 ml TiPB (12 mmol) and 2.41 mL of a 25% CTAC solution (1.83 mmol) were mixed in a 50 mL polypropylene reactor and heated to 60 °C under stirring in an oil bath.
Solution 2: was prepared in a 20 mL polypropylene reactor, containing 12.77 mL TEA (97 mmol) to which was added a premixed solution of 1.96 mL TEOS (8.8 mmol) combined with 0.2 mL APTES (0.86 mmol), for forming the core of the MSN particles. This solution was heated to 90 °C under static conditions for 1 h.
Solution 2 was added to solution 1 under strong stirring. The combined solutions were subsequently allowed to cool to room temperature under stirring. After 30 minutes we added, dropwise, the ingredients for the shell layer, consisting of a premixed solution of 22 µL MTES (0.11 mmol) and 22 µL TEOS (0.10 mmol). The condensation reaction was allowed to continue over night at room temperature.

Subsequently, this suspension was mixed with an additional 50 ml ethanol for 15 minutes, and the sample was collected by centrifugation. Template extraction was performed as described below. Samples with a lower degree of co-condensation with APTES were synthesized accordingly by adjusting the APTES amount in solution 2.

Changing the particle size (samples S-, M-, L-C):

In order to decrease the particle size (to about 50-60 nm) only 4.3 g of TEA were used in solution 2 while for increasing the particle size (to about 240 nm) 21.4 g TEA were used instead.

Inclusion of di- or tetra-sulfide groups into the pore walls
(samples M-C-S10, -30, -50; M-C-S(4)30, S-B-S(4)50 and S-N-S(4)50):

These samples were prepared as described above for the M-C samples, but 10, 30 or 50 mol % of TEOS in solution 2 was replaced by the bi-silane bis(3-triethoxysilylpropyl)disulfide (BTDS) to obtain

samples M-C-S-10, -30, -50:
Sample M-C-S10: 1.77 ml TEOS (7.95 mmol) and 0.209 g BTDS (0.44 mmol or 0.88 mmol Si)
Sample M-C-S30: 1.38 ml TEOS (6.19 mmol) and 0.627 g BTDS (1.32 mmol or 2.64 mmol Si)
Sample M-C-S50: 0.98 ml TEOS (4.40 mmol) and 1.045 g BTDS (2.20 mmol or 4.40 mmol Si)
For comparison we prepared also tetrasulfide-containing samples by replacing 50 mol % of TEOS with the bi-silane bis(3-triethoxysilylpropyl)tetrasulfide (BTES):
Sample M-C-S(4)50: 0.98 ml TEOS (4.40 mmol) and 1.19 g BTES (2.20 mmol or 4.40 mmol Si)
The samples were otherwise treated as described above.

MSN synthesis at neutral pH:

21.7 mL H_2O (1.12 mol), 2.97 ml TiPB (12 mmol), 2.41 mL of a 25% CTAC solution (1.83 mmol) and 0.1 g of TEA were mixed in a 100 mL round bottom flask (pH = 8) and heated to 95 °C. 1.96 mL TEOS (8.8 mmol) was added dropwise under stirring and the reaction was continued for 4 h, cooled down, and template extraction was performed as described below.

MSN synthesis at acidic conditions:
The synthesis of the siliceous LP-MSN nanoparticles was performed following a procedure similar to a previous report.[(28)]
1.4 g of the fluorocarbon surfactant was dissolved together with 0.5 g of the block copolymer surfactant F127 in 60 g of a 0.02 M HCl solution at 60 °C under stirring at 800 rpm for 2 hours. The solution was cooled down to 15 °C in a thermostat and 0.5 g of TMB was added as pore extension agent. This mixture was stirred for 2 hours before 3 g of TEOS were subsequently added under stirring, which was continued for 24 hours. Finally, the mixture was filled into a 100 mL Teflon-lined autoclave and heated under autogenous pressure at 150 °C for another 24 hours. The product was centrifuged after cooling at 20 000 rpm for 15 minutes and the supernatant was exchanged for 30 g of a 2 M HCl solution. A second heat treatment was performed for 2 days at 140°C.

Template extraction
Samples were retrieved by centrifugation and the supernatants were exchanged for 35 mL HCl/ethanolic extraction solution (10 mL concentrated HCl in 90 mL ethanol) and were refluxed at 90 °C for 45 minutes. This process was repeated once before the samples were washed 2 times in a 50 mL ethanol/water solution. Samples were finally stored at a concentration > 10 mg/mL in ethanol for further use.

Characterization of MSNs
Transmission electron microscopy (TEM) was performed on a Tecnai G2 20 S-Twin operated at 200 kV using a TemCam-F216 camera (TVIPS). A drop of an MSN-ethanol suspension was placed on a carbon-coated copper grid and dried at room temperature for several hours before TEM observation. Samples after various stages of dissolution in aqueous phase were centrifuged for 20 minutes, the residues were kept and redispersed by sonication in ethanol before TEM measurements. Nitrogen sorption measurements were performed on a Quantachrome NOVA 4000e Instrument at 77 K. Template-extracted MSN samples (about 15 mg) were degassed for 12 h at 120 °C under vacuum (10^{-5} Torr) before measurement. The pore volume and pore size distribution were calculated based on the NLDFT equilibrium and/or adsorption branch model for N_2 on silica. The hydrodynamic size distribution of MSNs was measured by dynamic light scattering (DLS) analysis using a Malvern Zetasizer-Nano instrument equipped with a 4 mW He-Ne laser (633 nm). Samples were measured

before and during the dissolution experiments. When measuring during the dissolution experiments the samples were either used as such or by using their supernatants retrieved after 20 minute centrifugation. Zeta potentials were measured with an attached multi-purpose titrator. FTIR spectra of KBr-pelleted MSN samples and Raman spectra of pure MSN powders were recorded on a Bruker Equinox 55 IR instrument equipped with a FRA 106/s Raman module using a LN_2 cooled Ge detector and an Nd:YAG 1064 cm^{-1} laser. UV-VIS spectra of supernatants were recorded in transmission on a Perkin Elmer Lambda 1050 instrument in disposable 1 cm PMMA cuvettes. ^{29}Si cross-polarized (CP) and direct-polarized (DP) solid state magic angle spinning SS-MAS NMR measurements were performed on a Bruker Avance III-500 (500 MHz, 11.74 T) with a spinning rate of 10 kHz. About 100 mg MSN samples were used in 4 mm ZrO_2 rotors with reference to tetramethylsilane (TMS). For CP: contact time 4 ms, pulse length 2.5 µs, scan delay 0.5 s, number of scans about 5000; DP: scan delay 512 s, number of scans about 128.

Covalent attachments

PEGylation: polyethylene glycol was covalently attached via a maleimide linker to the mercapto groups in the shell of MSNs by using a molar ratio of 1:2 SH : MAL-PEG-OMe. 200 µL of a MAL-PEG(750)-OMe stock solution containing 16.5 mmol PEG/mL were added to 10 mg MSN and were refilled to 1 mL and sonicated for 1 minute. The samples were shaken at 37 °C for 1 h and separated from excess PEG by centrifugation and repeated washing. Samples were stored as 10 mg MSN-PEG /mL ethanol until further use.

ATTO-in: 1 mg ATTO-488 NHS ester was dissolved in 400 µL dry DMF to result in a slightly reddish solution. 10 µL of this solution were added to 3 mg MSN dissolved in 1mL ethanol and were reacted under exclusion of light for 1 h under shaking at 37 °C. Three washing cycles with 1 mL ethanol were subsequently performed to remove unreacted dye from the sample. Samples were diluted in 30 mL buffer or water and were stirred at 37 °C under exclusion of light. Aliquots were taken off after specific time intervals, centrifuged and supernatants were kept for analysis with ICP and UV-VIS.

ATTO-in/out, ATTOin/PEGout: 2 mg MSN-ATTOin were prepared in 1 ml ethanol as described above. This sample was subsequently divided into 2 x 500 µl aliquots (1 mg MSN each). 5 µL of an ATTO-633 maleimide solution (1 mg ATTO-633 dissolved in 400 µL dry DMF) were added to one aliquot (ATTOin/out). To the other aliquot we added 20 µl of an aqueous solution of a 12 mg/mL MAL-PEG(7500) **s**tock solution (ATTOin/PEGout). Both samples were shaken at RT for 1 h under exclusion of light.

Biotin/avidin coupling: aliquots of 1 mg of ATTOin MSN samples in ethanol were exposed to 50 µl of an HPDP-biotin solution (4 mM solution in DMF) and shaken at room temperature under the exclusion of light for 1 h. Some aliquots were further used for adding 0.5 mL avidin (1mg/mL water) to the biotin functionalized sample and shaking was continued for 1 additional hour.

DOTAP lipid layer: another ATTO-in aliquot was used for a lipid layer enclosure. 200 µL of a DOTAP solution (6.25 mg DOTAP in 40:60 vol ratio of EtOH:water) was mixed with a cake of 2 mg of ATTOin MSN by carefully pipetting the sample up and down and subsequently 1.3 mL of 4°C cold water was added to instantaneously form the lipid bilayer.

All of the above samples were washed with ethanol and water before use in the dissolution experiments.

Dissolution experiments:

Stock solutions with a concentration of 1 mg/mL of pristine MSN samples or covalently functionalized MSN samples were prepared. Aliquots of each MSN sample were prepared in triplicates for each data point by adding 200 µl to 1.8 mL of either a buffer solution or water to achieve a concentration of 0.1 mg MSN/mL. These aliquots were filled into 2 mL Eppendorf tubes (Epis). After short vortexing, samples were shaken at 37 °C at 500 rpm for extended times as mentioned in the figure captions. Epis were removed from the shaker after certain intervals and centrifuged for 20 minutes at 16873 rcf. Supernatants were carefully taken off by pipette and 1 mL of the supernatant of each sample was analyzed by ICP. The solid residues of selected samples were redispersed in ethanol for subsequent TEM analysis.

ICP analysis:

ICP (Inductively Coupled Plasma - Optical Emission Spectrometry) measurements were performed with an ICP OES (Varian Vista RL) instrument. Each data point was measured in triplicate and automatically averaged. Each sample for dissolution experiments was prepared in triplicate and used for statistical analysis. Liquid samples were measured after appropriate dilution and referenced against a blank, either water or the respective buffer solution. Solid parent samples of the different MSNs were dissolved in HF and measured with ICP after appropriate dilution. The Si content in mg/mL obtained from these solid samples was taken as 100 % reference for the dissolved Si content in the supernatants.

Table S-2: Overview over synthesis conditions and chemical properties of samples

Sample	Coconden-sation % of total silica	TEOS : TEA	Particle size TEM (nm)	BET surface area (m^2/g)	Pore volume mL/g at 0.8 (p/p_0)	Pore size Ads. branch (nm)	Synthesis condition
S-C	9% NH_2in 1% SH out	1 : 3	50-70	722	0.60	4.8	basic
M-C	9% NH_2in 1% SH out	1 : 10	110	694	0.66	4.8	basic
L-C	9% NH_2in 1% SH out	1 : 15	240	681	0.64	4.6	basic
L-C-6%	6% NH_2in 1% SH out	1 : 10	110	860	0.84	4.5	basic
M-C-Ph	1% Ph in 2% SH out	1 : 5		965	1.09	5.3	basic
Si-N	Pure silica	1 : 0.07	60-70	540	0.55	4.6	neutral
Si-B	Pure silica	1 : 10	70-120	1130	1.38	4.8	basic
Si-A	Pure silica	-	100-300	306	0.81	7-12	acidic
M-C-S10	9% NH_2in 1% SH out 5% BTDS	1 : 10	100-150	892	0.71	4.5	basic
S-C-S10	9% NH_2in 1% SH out 5% BTDS	1 : 3	60-80	483	0.38	4.8	basic
M-C-S30	9% NH_2in 1% SH out 15% BTDS	1 : 10	70-100	712	0.51	4.4	basic
S-C-S(4)30	9% NH_2in 1% SH out 15% BTES	1 : 5	70-100	378	0.6/0.38	3.6	basic
M-C-S50	9% NH_2in 1% SH out 25% BTDS	1 : 10	70-100	290	0.54/0.17	4.4	basic

S = small particle size, M= medium particle size, L large particle size, C = co-condensed, NH_2 = 3-aminopropyltriethoxysilane (APTES), SH = (3-mercaptopropyl)triethoxysilane (MTES), Ph =

phenyltriethoxysilane, Si = pure silica samples without co-condensation, B = basic conditions, N = neutral conditions, A = acidic conditions

The pore volume was evaluated up to the relative pressure of 0.8 in order to exclude textural pores from particle packing.

Table S-3: Overview over synthesis conditions and chemical properties of samples containing disulfide groups

Sample	Coconden sation % of total silica	TEOS : TEA Mol%	Particle size TEM (nm)	BET surface area (m^2/g)	Pore volume mL/g at 0.8 (p/p_0)	Pore size Ads. branch (nm)	Synthesis condition
M-C-S10	9% NH_2in 1% SH out 5% BTDS	1 : 10	100-150	892	0.71	4.5	basic
S-C-S10	As above	1 : 3	60-80	483	0.38	4.8	basic
M-C-S30	9% NH_2in 1% SH out 15% BTDS	1 : 10	70-100	712	0.51	4.4	basic
S-C-S(4)30	As above but 15% BTES	1 : 5	60	378	0.38	3.6	basic
M-C-S50	9% NH_2in 1% SH out 25% BTDS	1 : 10	70-100	290	0.17	4.4	basic
Si-B-S(4)50	No co-cond. 25% BTES	1 : 5	50	540	0.54	4.2	basic
Si-N-S(4)50	No co-cond. 25% BTES	1 : 0.07	30-40	250	0.29	5.9	neutral

S = small particle size, M= medium particle size, L large particle size, C = co-condensed, NH_2 = 3-aminopropyltriethoxysilane (APTES), SH = (3-mercaptopropyl)triethoxysilane (MTES), Si = pure silica samples without co-condensation other than sulfide-containing silanes, B = basic conditions, N = neutral conditions,
BTDS = bis(3-triethoxysilylpropyl)disulfide (S), BTES = bis(3-triethoxysilylpropyl)tetrasulfide (S4).

The pore volume was evaluated up to the relative pressure of 0.8 in order to exclude textural pores from particle packing.

Figure S-1: Long-term shelf-life of MSNs - BET

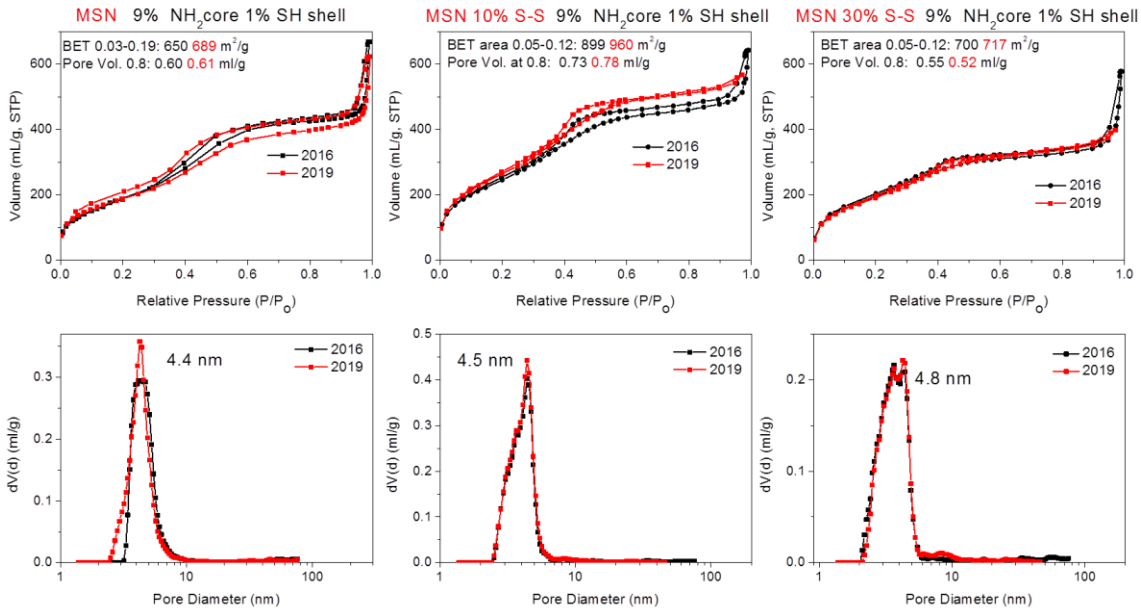

Figure S-1:
Comparison of surface properties of samples stored for over 3 years:
Compilation of nitrogen-sorption isotherms (top) and corresponding pore-size distributions of representative MSN samples prepared via the co-condensation method as described under MSN synthesis at basic pH. Shown are samples containing 9% amino- groups in the core of the particles and 1% mercapto-groups in the shell of the particles (M-C, left) as well as particles containing additionally either 10 % or 30 % of disulfide groups (M-C-S10, M-C-S30, middle and right). When stored in ethanolic solutions at concentrations larger than 10 mg/mL we did not observe indicative changes for structural degradation after this long storage time.

Figure S-2: Long-term shelf-life of MSNs – TEM and DLS

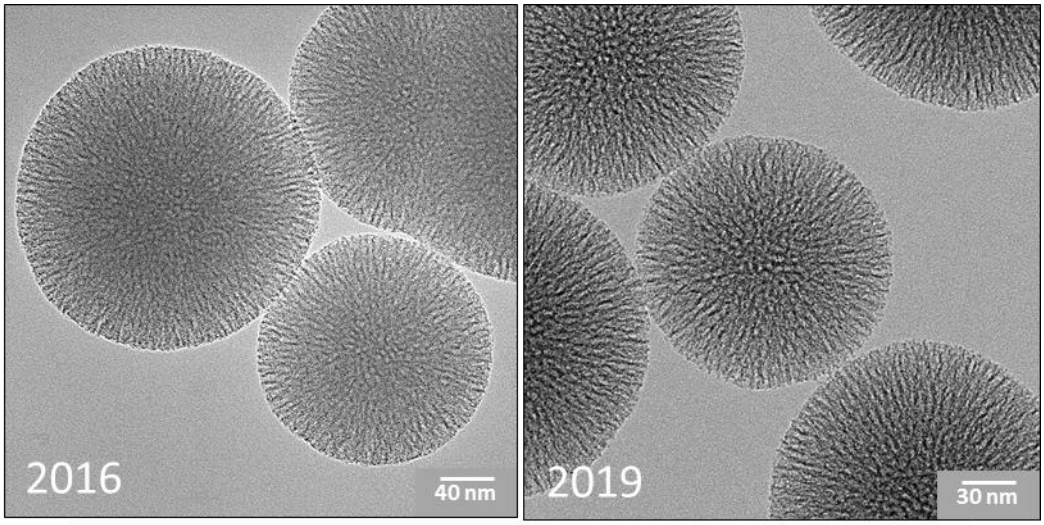

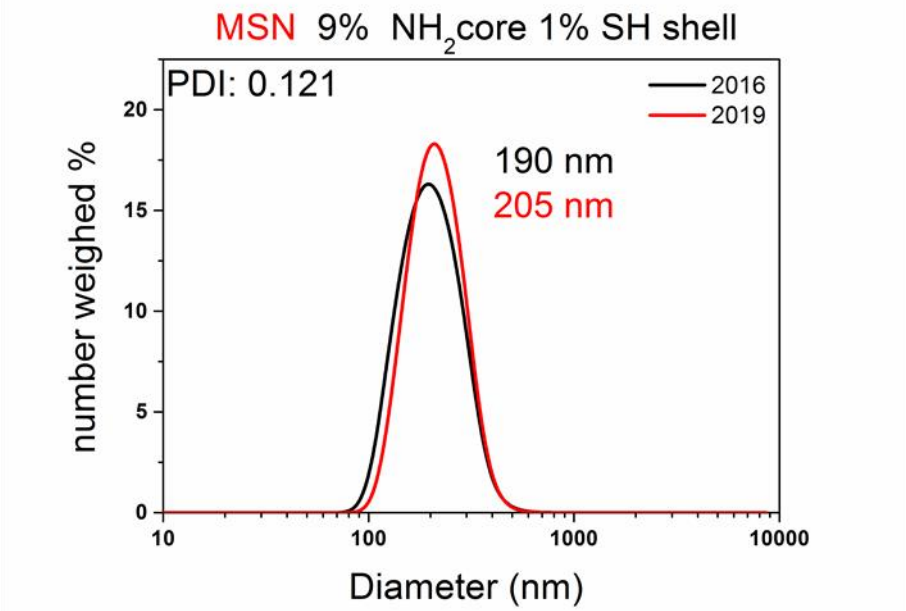

Figure S-2:
TEM (top) and corresponding particle size distributions obtained by DLS in water (bottom) of a representative MSN sample M-C prepared via the co-condensation method as described under MSN synthesis at basic pH before and after 3 years of storage in ethanol.

Figure S-3: Change of particle size and reproducibility

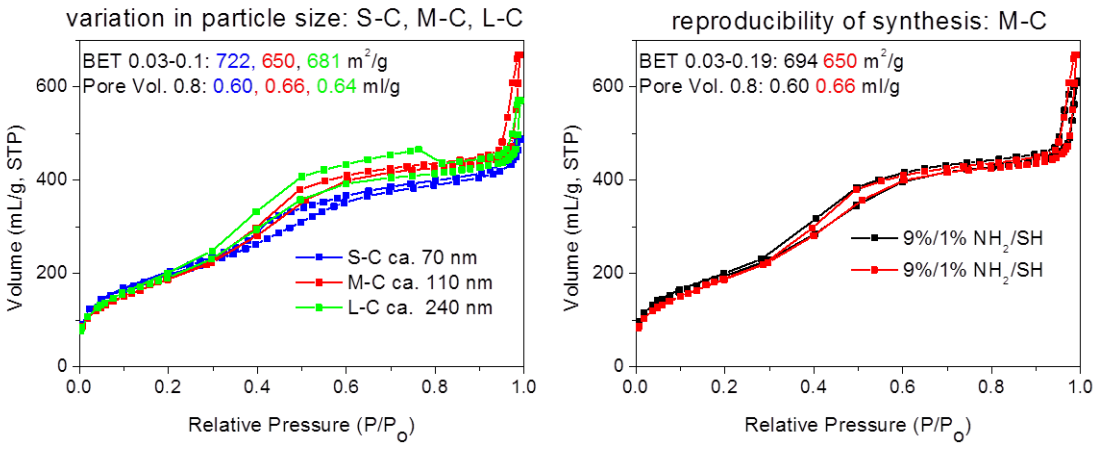

Figure S-3:

Left: Nitrogen sorption isotherms of co-condensed MSN samples prepared under basic reaction conditions with varying ratios of TEOS : TEA in order to create particles of different sizes, small (S-C), medium (M-C) and large (L-C).

Right: documentation of the synthesis reproducibility. Both samples shown were prepared following the same basic recipe under co-condensation of 9% amino groups in the core and 1% mercapto-groups in the shell.

Figure S-4: TEM and EDX data of dissolution residues of sample M-C

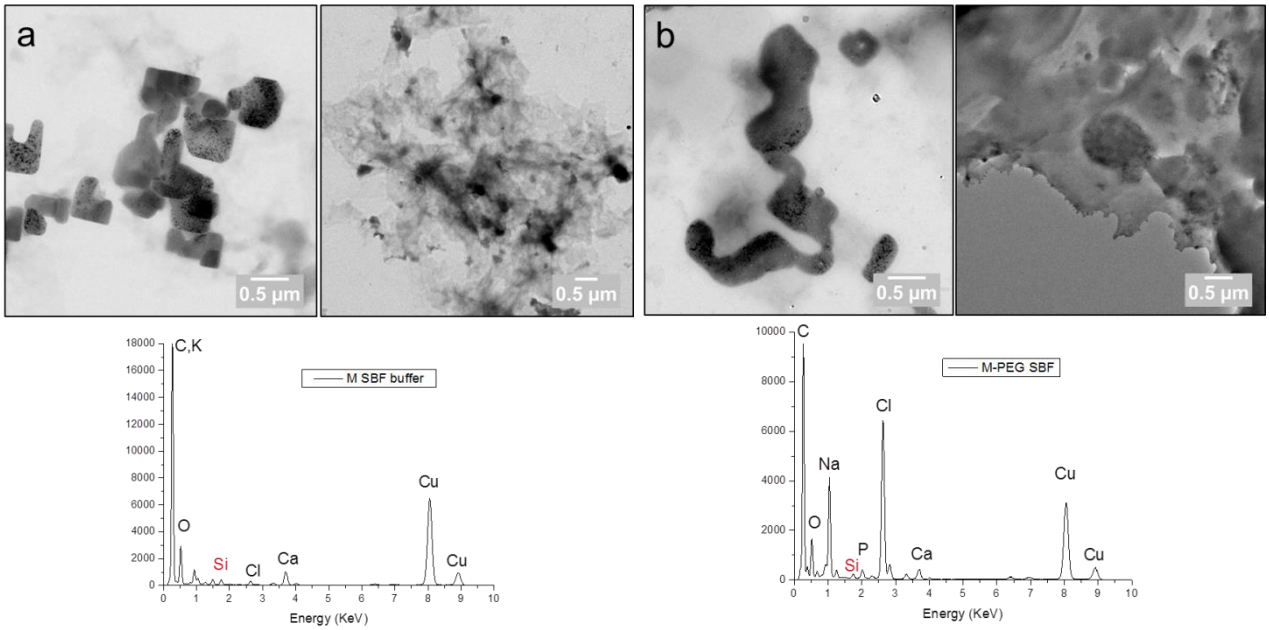

Figure S-4: TEM and corresponding EDX data of residues found in sample M-C of Figure 2 in the manuscript after stirring in SBF buffer for prolonged time. Samples were centrifuged for 45 minutes, the supernatant was removed and the remaining solid was redispersed in ethanol.
a) residues of sample M-C after 2d, the corresponding EDX (bottom) was taken from the area in the right micrograph
b) residues of sample sample M-C-PEGout after 5 d, the corresponding EDX (bottom) was taken from the right micrograph.

These TEM and EDX measurements show that only salt residues from the buffer solution are present in the solid residues following the dissolution experiments. Without performing EDX measurements these residues could have been mistaken for silica residues instead. Since these salts may obscure the visual inspection for any possible silica degradation residues, we performed most of the dissolution studies in water under exclusion of salts. As seen in Figure 2c) in the manuscript, we have established that the degradation is independent of the presence of salt in the dissolution medium.

Figure S-5: TEM micrographs of residues of sample M-C-ATTOin and DLS of supernatants

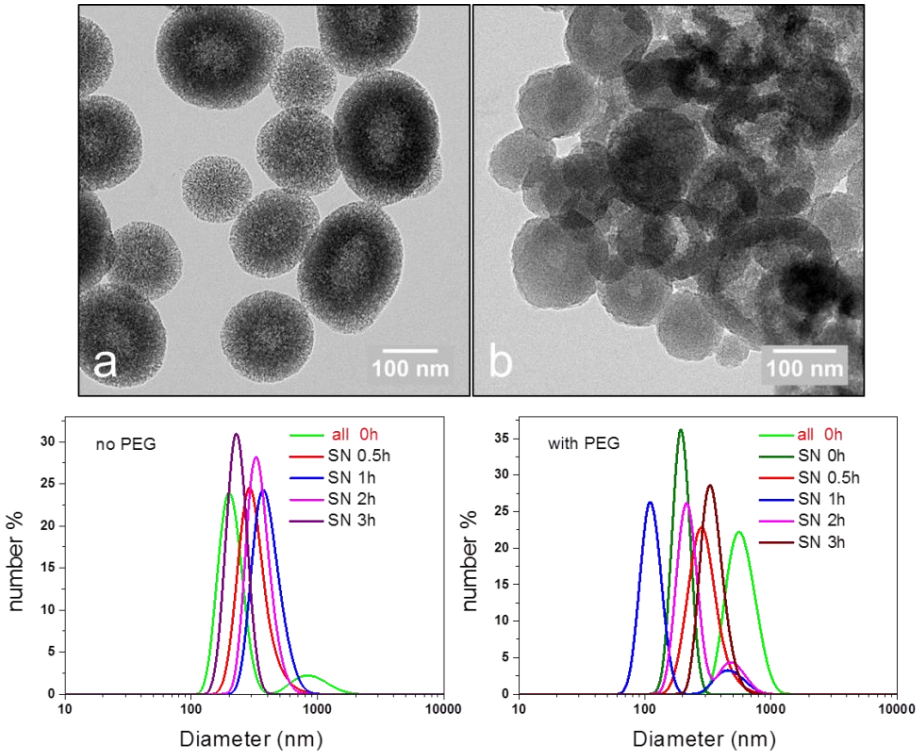

Figure S-5:

Top: TEM micrographs of solid residues of sample M-C-ATTOin after a) 1 h and b) 3 h stirring at 37 °C in salt-free water. Most of the porous structure of the parent sample has nearly vanished after 1 h stirring and has completely densified after 3 h.
Bottom: DLS spectra of MSN solutions of M-C-ATTOin and sample M-C-ATTOin/PEGout. Light green: DLS of the samples at the start of the dissolution experiment (all, t = 0 h), SN: retrieved supernatants after 20 minutes of centrifugation, obtained after different time intervals of stirring at 37 °C.

Measurements of the supernatants required an extremely high instrumental amplification, thus only spurious particles are still detected in the solution. These DLS spectra are only shown to document that essentially all remaining solids are removed from the supernatants and furthermore, that no small fragments (<< 100 nm) of the silica particles remained in solution after centrifugation.

Figure S-6: Influence of MSN concentration ranging from 0.1 mg/mL to 0.4 mg/mL in sample M-C-ATTOin

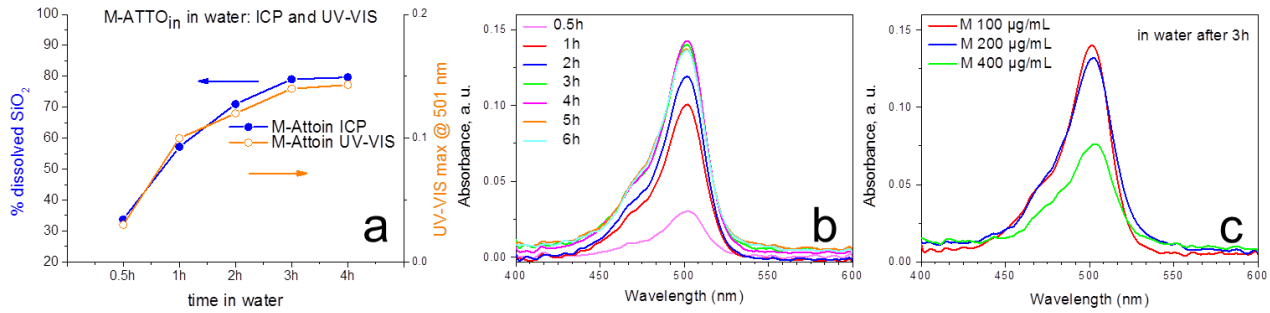

Figure S-6: UV-VIS analysis of ATTO-labeled sample M-C-ATTOin after degradation in water
a) overlay of ICP results and UV-VIS maximum intensity of dye-containing supernatants as a function of time,
b) corresponding UV-VIS spectra of sample M-C-ATTOin,
c) UV-VIS spectra of concentration-dependent dissolution of sample M-C-ATTOin after 3 h using 0.1 mg/mL, 0.2 mg/mL and 0.4 mg/mL MSN concentrations.

Fig. S-6a: ICP and UV-VIS data follow the same time trend, indicating a dissolution process that is dominated by hydrolysis of the inner particle surface. The corresponding spectra in Fig. S-6b show the UV-VIS absorption of dye released through the dissolution of sample M-C-ATTOin, reaching a maximum after 3-4 hours at which time 80% of the sample was found to be dissolved (by ICP).
Fig. S-6c shows the concentration-dependent dissolution. By doubling the MSN concentration to 0.2 mg/mL (blue curve) we find similar amounts of dye released as in the 0.1 mg/mL sample, while with a 4-fold concentration (0.4 mg/mL, green curve) we find only about 50 % of dye in the supernatant after 3 h. This documents that the dissolution process is highly dependent on the sample concentration.

Figure S-7: TEM micrographs and DLS measurements of purely siliceous samples prepared at different pH

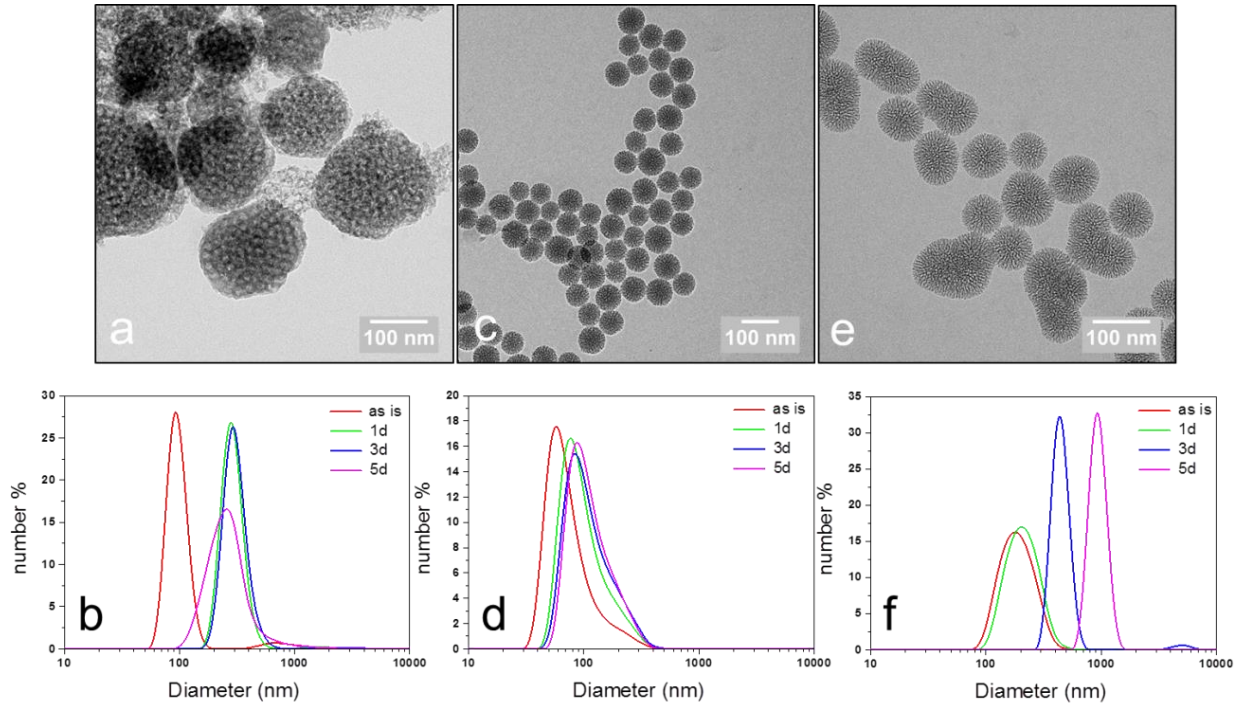

Figure S-7: TEM micrographs (top) and DLS measurements (bottom) of samples a, b) Si-A (acidic pH synthesis), c, d) Si-N (neutral pH synthesis), e, f) Si-B (basic synthesis). TEM pictures were taken before starting the dissolution experiments, DLS measurements were performed before (red) and during dissolution experiments with samples in water. All siliceous samples showed a high stability even after prolonged time of stirring at 37 °C; the most stable sample in DLS is Si-N (Figure 7 d), while samples Si-A (Figure 7 b) and Si-B (Figure 7 f) started to show signs of agglomeration with time.

Figure S-8: TEM micrographs of morphology changes of siliceous sample Si-B (basic pH) during dissolution

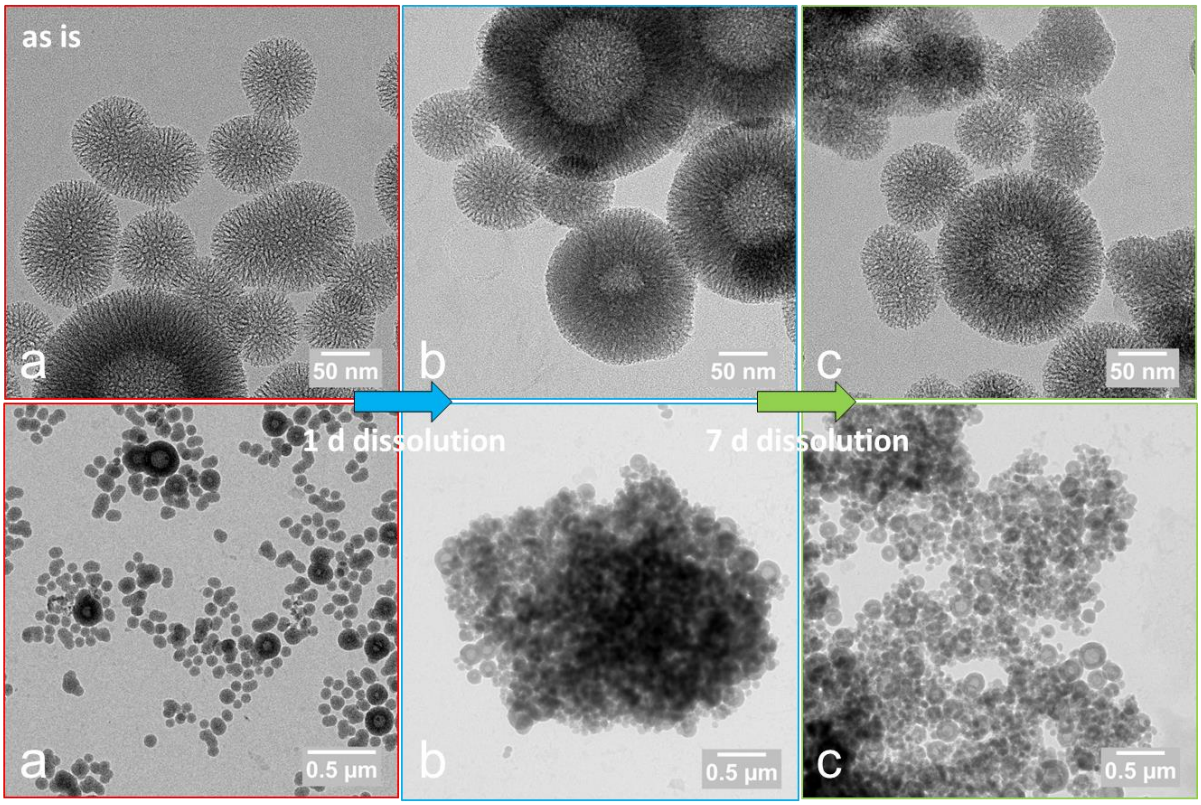

Figure S-8: TEM micrographs of siliceous sample Si-B made at basic pH, a) before and b) after 1 d, c) after 7 d stirring in water at 37 °C.

This sample shows a higher resistance against degradation and morphology changes than the co-condensed samples but is more sensitive than the samples made under neutral pH. A few doughnut-like particles are already present here in the starting material; however, stirring for prolonged time in water transforms nearly all particles into these shapes, but the pore structure is still visible even after 7 d.

Figure S-9: FT-Raman spectroscopy of co-condensed samples M-C and M-C-S with S-S inclusion

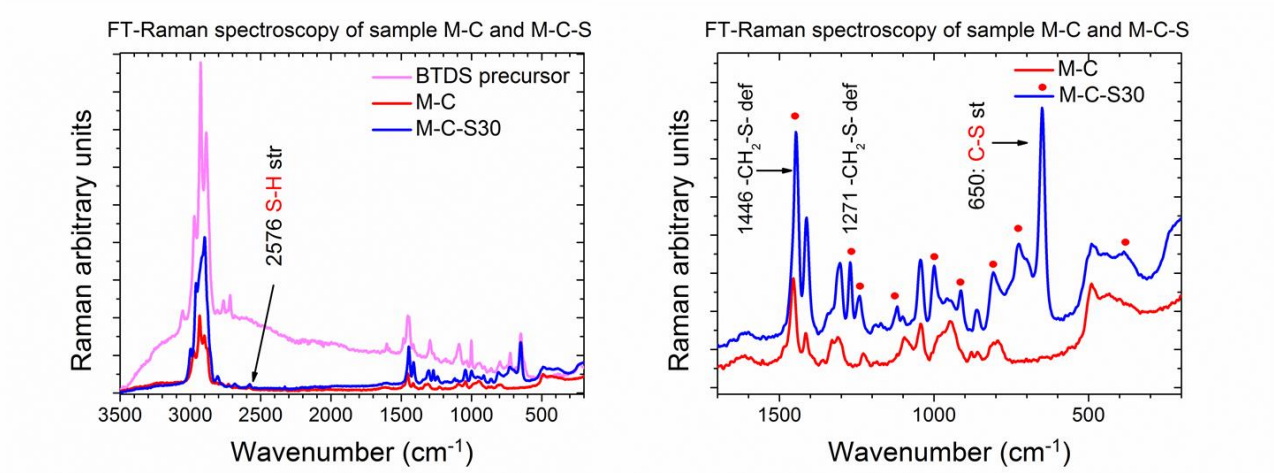

Figure S9: FT-Raman spectroscopy of co-condensed samples M-C without S-S inclusion (red) and co-condensed sample M-C-S30 in which 30% of the silica content was replaced by the disulfide BTDS (bis-[(triethoxysilyl)propyl]disulfide; blue),
left: full spectrum, including the precursor BTDS;
right: zoom into the low wavenumber region. The terminal mercapto goup of these NH_2in/SHout co-condensed samples is visible in both MSN samples at 2576 cm^{-1} (left) while additional vibrations in M-C-S30 indicate the inclusion of the BTDS (right). Prominent bands are labelled and new bands in M-C-S30, when compared to the parent sample M-C, are marked by a red dot. The band at 1446 is shifted by 10 wavenumbers in comparison to the aminopropyl residue in the parent sample M-C (1456 cm^{-1}).

Figure S-10: ICP measurements comparing sample M-C and S-S containing samples M-C-S10, M-C-S30, as well as S-C-S(4)30

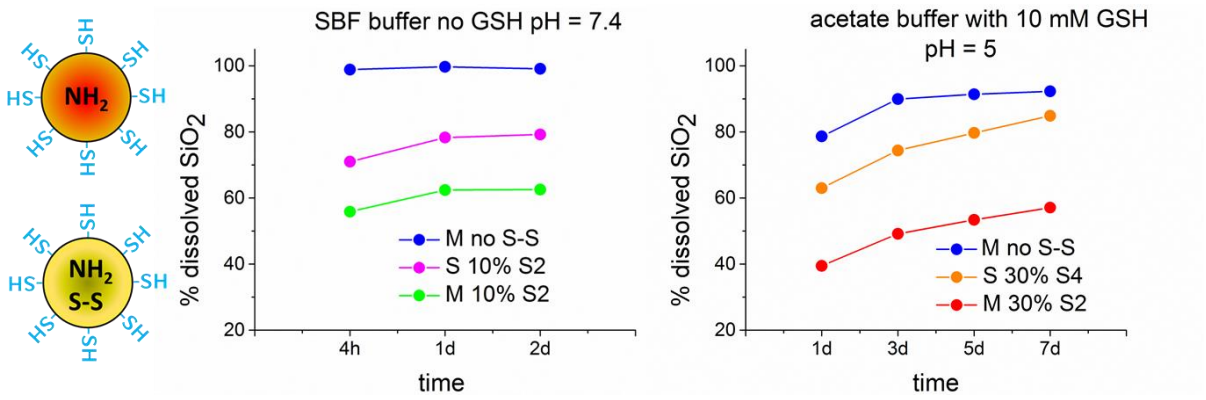

Figure S-10 left: ICP measurements comparing the parent co-condensed sample M-C and the 10% S-S sample M-C-S10 in SBF at pH = 7.4 from 4 h to 2 days, confirming a retardation of the dissolution process in the presence of disulfide groups. We have included measurements on a smaller-sized 10 % containing S-S sample (S-C-S10) with a particle size of about 70 nm as compared to about 110 nm for samples M-C.

Figure S-10 right: Dissolution behavior in the presence of the reducing agent GSH (10 mM) in acetate buffer at pH = 5 over long time periods of up to 7 days. The parent sample M-C is compared to medium-sized sample M-C-S30 and small-sized sample S-C-S(4)-30. The latter sample was co-condensed with 9 % amino groups in addition to 15 % of the tetrasulfide bis-silane BTES. Only this sample shows a dissolution degree close to the parent sample M-C containing no disulfide groups. The sample M-C-S30 containing 30 % disulfide groups is dissolved to only 50 % even under reducing conditions after 7 days.

Figure S-11: TEM degradation studies of S-S containing samples

The slow degradation of the S-S samples was further confirmed by TEM analysis after different time periods (Fig. **S11 to S13**). Structural changes in the form of densification and partial loss of pore structure are already visible after 1 h in the parent sample M-C, while the onset of this process is delayed in the S-S samples. Furthermore, we do not observe a breakdown of the S-S samples into fragments upon GSH treatment in the TEM or by DLS; here we observe a transformation into gel-like residues after 8 days (see Fig. **S-13**). Similar agglomerates were shown by Huang et al.[(24)] in TEM micrographs of comparable particles treated for 7 days in SBF under the influence of 10 mM GSH. They found a nearly complete disintegration into small substructures by TEM only upon prolonged exposure for 14 days. We note that most of our samples were studied in water to avoid misleading salt interferences in the TEM analysis.

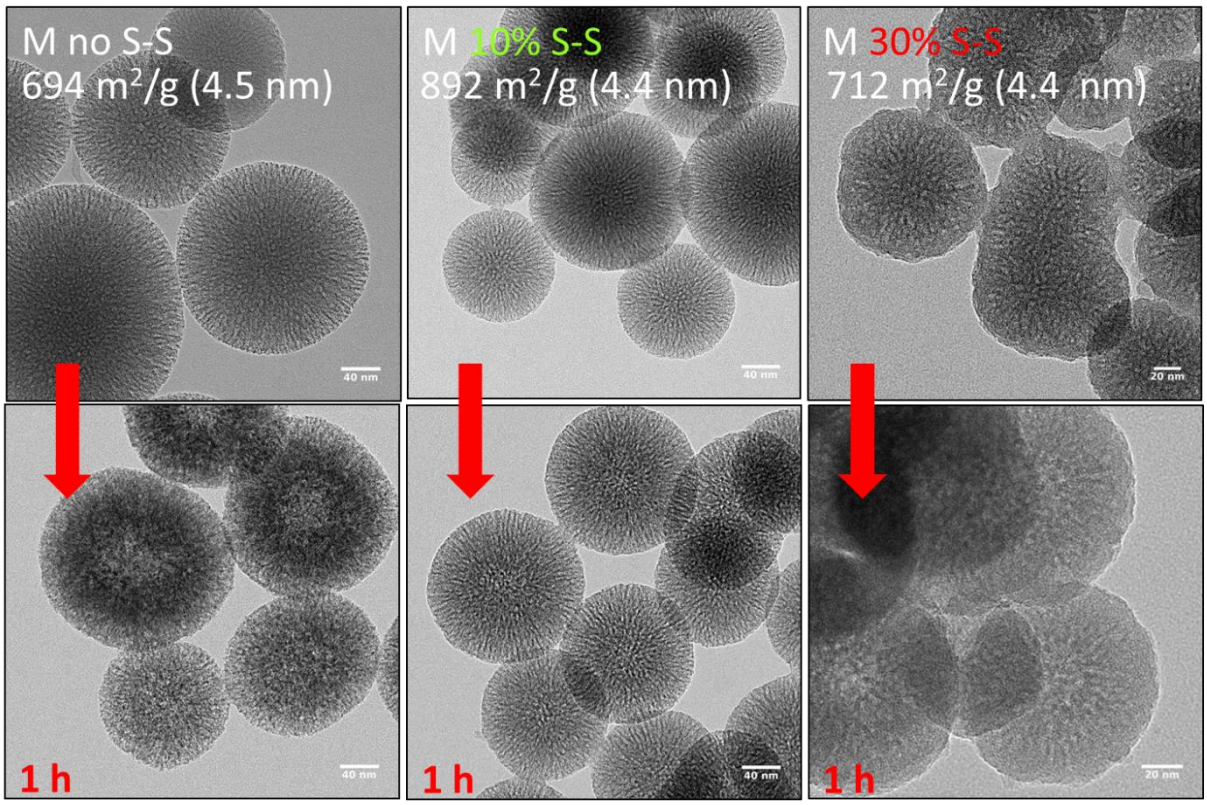

Figure S-11: TEM micrographs of co-condensed samples, M-C without inclusion of bis-[(triethoxysilyl) propyl] disulfide (BTDS, S-S), left column, and with 10% (M-C-S10) and 30% (M-C-S30) replacement of TEOS with S-S, shown in the middle and right column, respectively. Top row: samples before degradation, showing the surface area and pore sizes of the respective samples. Bottom row: samples after stirring in water at room temperature for 1 h (0.1 mg/mL). Morphological changes are only visible for the samples without S-S in the pore walls after this time at low concentration. The radial pore structure seems to be lost and a densification process is seen in a typical 'ring-formation' in the particle.

Figure S-12: Continuation of Figure S-11
TEM degradation studies comparing M-C and M-C-S10 and M-C-S30 after 3 h and after GSH exposure

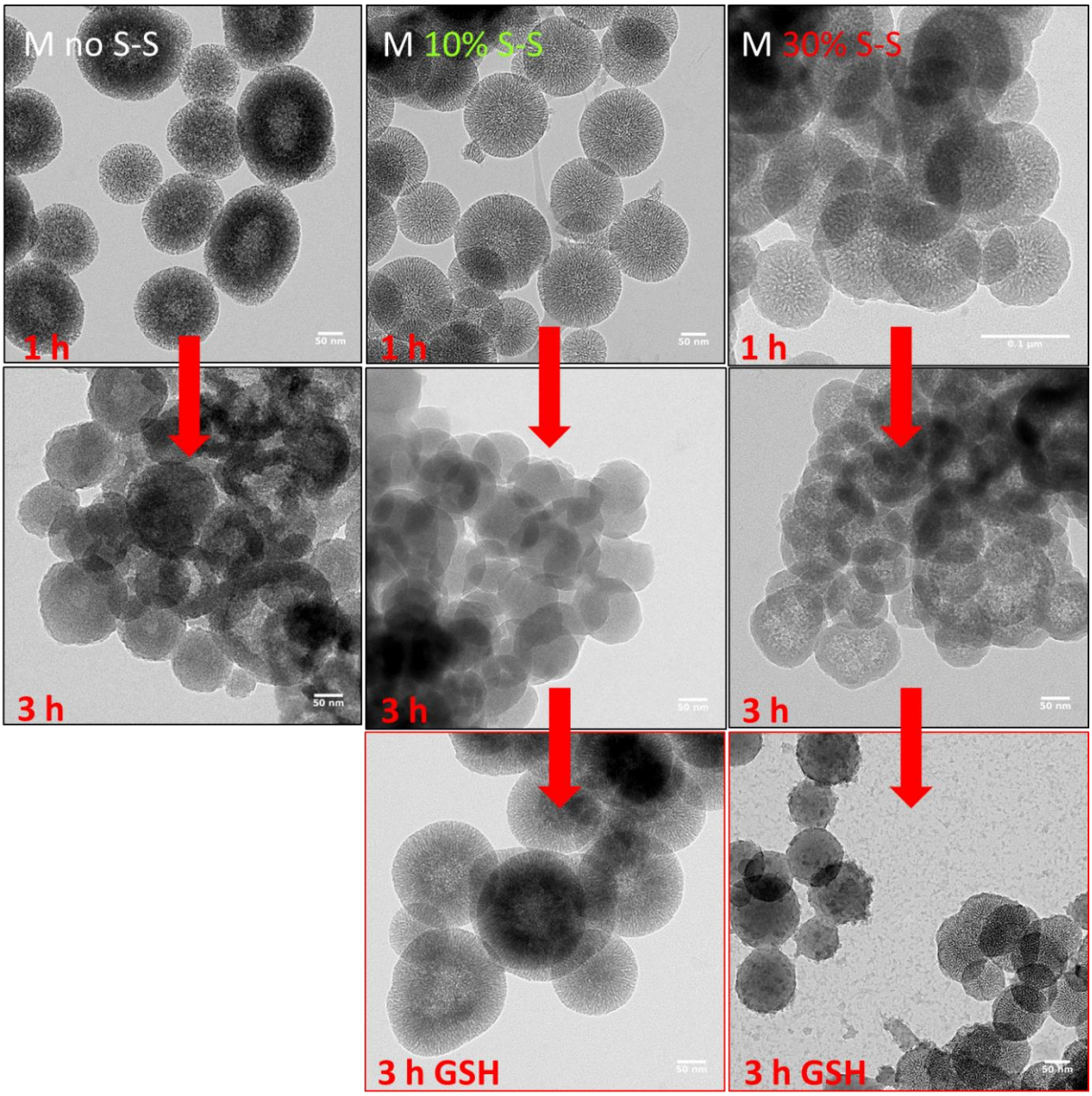

Figure S-12: TEM micrographs of co-condensed samples as in Figure S-11.
Top row: again for comparison samples M-C, M-C-S10 and M-C-S30 after stirring in water for 1 h.
Middle row: samples after stirring in water for 3 h.
Bottom row: S-S containing samples M-C-S10 and M-C-S30 after stirring for 3 h in 10 mM GSH PBS solutions. After 3 h all samples show a rearranged silica structure where the pore architecture is obscured while their spherical appearance is still retained. Samples with 10 % and 30 % S-S are also not disintegrated after 3 h in a reducing GSH solution; the small structures seen on the bottom row right are due to salt formation from PBS residues or carbon from the TEM grid, as indicated by EDX on several pictures. This sample M-C-S30 starts to lose the spherical structure after 10 days in GSH, forming a gel-like residue as seen below in Figure 13.

Figure S-13: TEM micrographs of sample M-C-S30 after 10 days in GSH

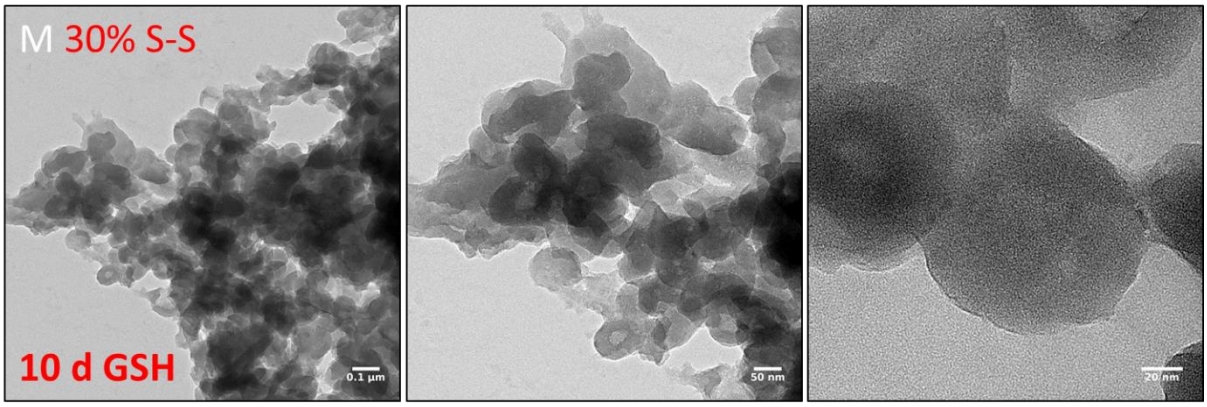

Figure S-13: TEM micrographs of co-condensed sample M-C-S30 with 30 % S-S, here after 10 days in PBS containing GSH at pH = 6.2. ICP results of these samples up to 7 days were shown in Figure S-10.

Figure S-14: UV-VIS degradation studies of S-S-containing samples

Similar to the approach illustrated in the manuscript in Figure 4, we followed the dissolution of the M-C-S samples by UV-VIS spectroscopy by covalently coupling an ATTO-dye to the internal amino groups. One part of the sample was exposed to water and comparable aliquots were exposed to a buffered solution containing GSH (see Figure **S-14** below). As observed before with ICP measurements, our results confirm that under non-reducing conditions smaller amounts of dye are released with increasing S-S content, pointing to a slower dissolution of disulfide samples than the parent M-C samples without S-S. However, in the presence of GSH we note a slight increase of degradation in the S-S samples, indicating that the disulfide groups possibly do undergo a partial fragmentation from the host lattice under reducing conditions.

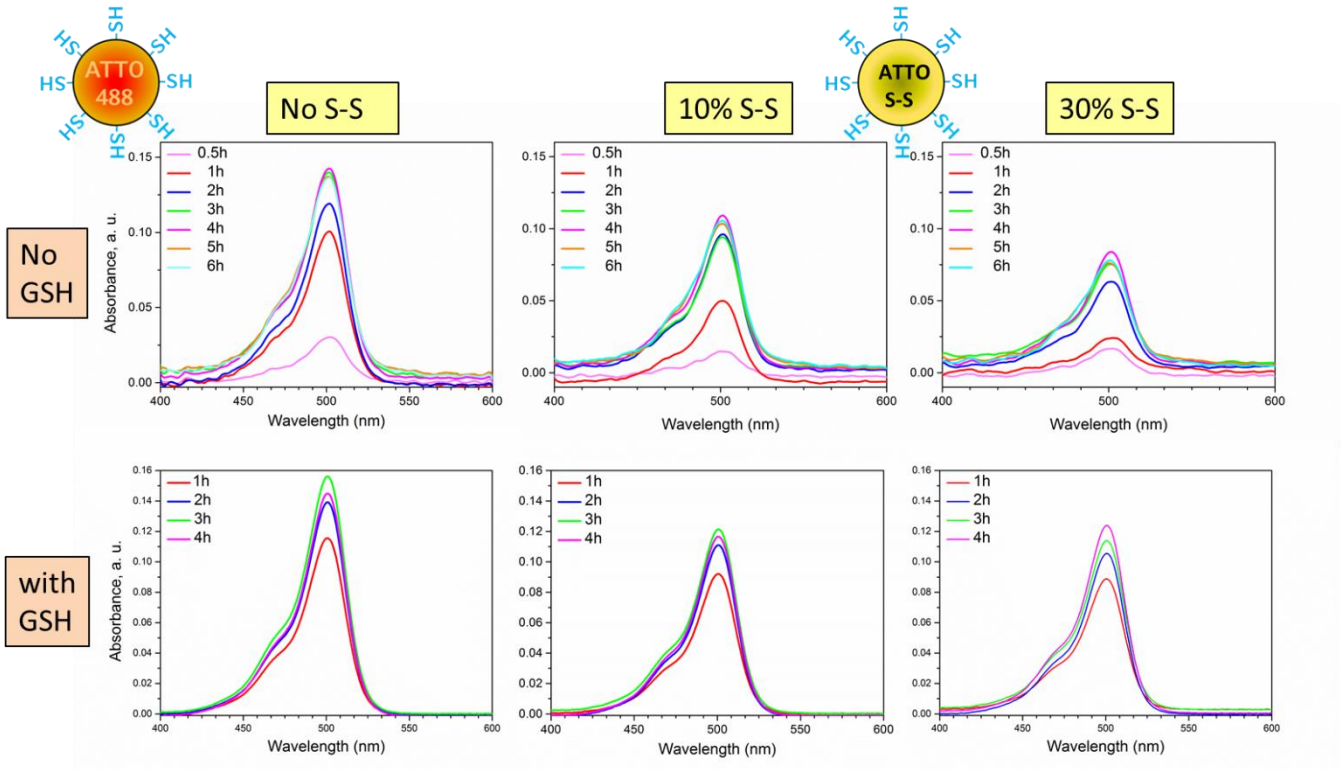

Figure S-14: Samples M-C (left column), M-C-S10 (middle column) as well as M-C-S30 (right column) were covalently labeled with an Atto dye via internal amino-groups. The enrichment of this dye in the supernatants was followed in time via UV-VIS spectroscopy using an MSN concentration of 0.1 mg/mL either in water (top row) or in a PBS solution containing 10 mM GSH at pH = 6.2 (bottom row). While a decreasing concentration of dye in the supernatant was observed with increasing S-S content in the sample (top row) we find a nearly identical dye concentration for the S-S samples under reducing conditions. This might indicate a partial S-S breakage and increased hydrolytic degradation. Samples in each column were prepared from identical stock solutions and measured on the same day.

Figure S-15: TEM and Raman studies on samples Si-B-S(4)50 and Si-N-S(4)50

To further investigate if a bond breakage of disulfide linkers might occur under reducing conditions, we prepared silica samples that contained just the larger S4-linkers in the lattice, since these were shown before by ICP to be most sensitive to reduction (see Figure S-10). Here, we did not include any additional co-condensation of amino- and mercapto-groups as usual in order to be able to detect the formation of internal –SH residues by Raman spectroscopy. Samples with the highest concentration of tetra-sulfides in the synthesis solution (replacement of 50 % of TEOS) were stirred for 7 days in DTT (0.1 mg/mL) and analyzed by TEM and Raman spectroscopy (see Figure **S-15** below). The TEM pictures demonstrate the retention of the porous particle structure, however no fragmentation as observed by other authors.[17, 20] A slight change in morphology is noticeable, likely a consequence of a partial bond cleavage as indicated by the strong S-H vibration detected in the Raman spectrum after this DTT treatment.

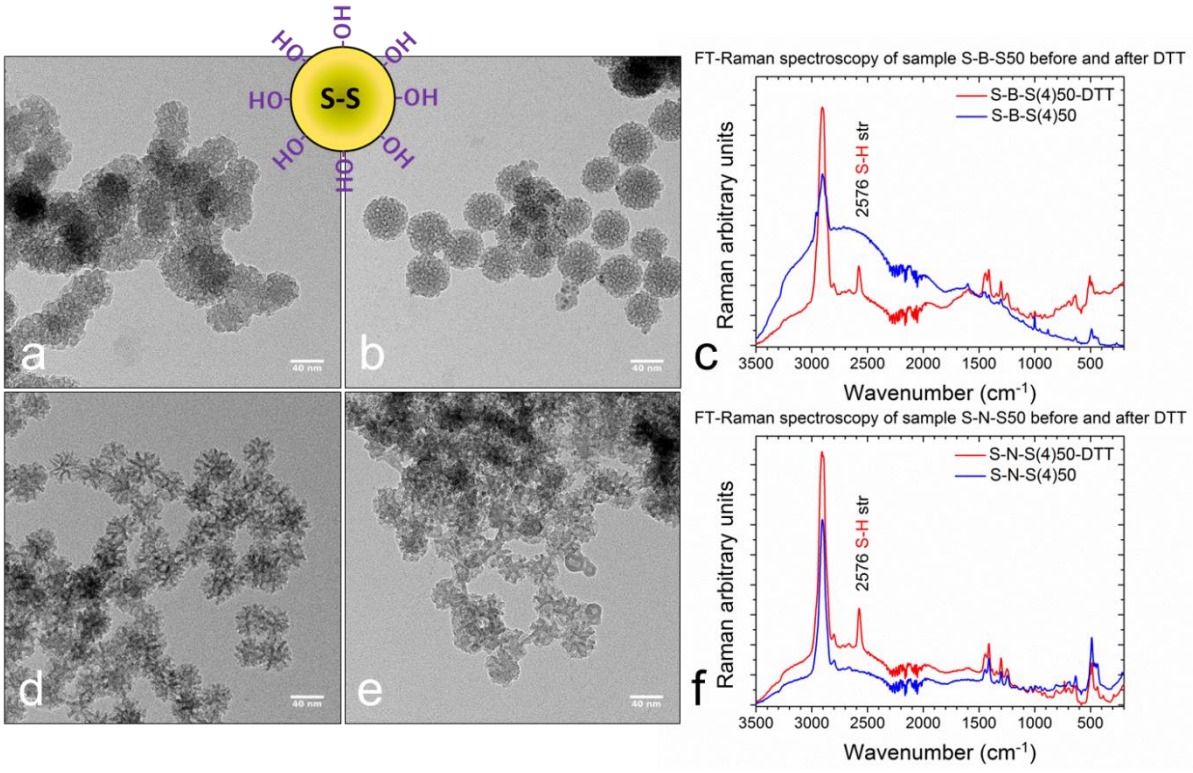

Figure S-15: Degradation of samples containing 50 % tetrasulfide in the lattice, Si-B-S(4)50 prepared under basic conditions (a-c) and Si-N-S(4)50 prepared under neutral conditions (d-f).
Panels a,d show TEM pictures before and panels b, e after stirring in DTT for 7 days. The corresponding Raman spectra show the generation of mercapto groups after this treatment, indicating some S-S bond-breakage.

Figure S-16: UV-VIS degradation studies as function of concentration of samples M-C, M-C-S10 and M-C-S30

We also used UV-Vis spectroscopy to study the significant influence of MSN concentration on the dissolution rate by comparing concentrations of 0.1, 0.2 and 0.4 mg MSN/mL after stirring for 3 hours (see Figure **S-16** below). For comparison we included the parent sample M-C. As shown before this sample displays a strong sensitivity for dissolution even at higher concentrations. At 0.4 mg/mL we notice a substantial resistance against dissolution. This behavior is further retarded by S-S inclusion into the MSN: while sample M-C-S10 shows a continuous decrease of dissolution with increasing concentration, there is nearly no elution of dye when the concentration is decreased from 0.4 mg/mL to 0.2 mg/mL in sample M-C-S30, and only at the lowest concentration we observe substantial dissolution.

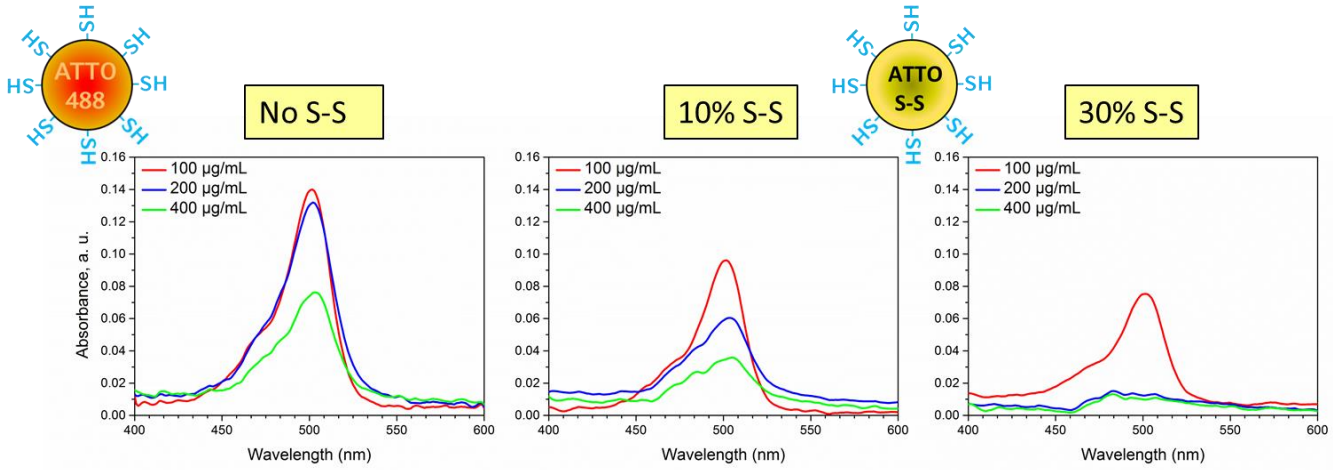

Figure S-16: UV-VIS dissolution measurements as a function of particle concentration of ATTOin-labeled samples as displayed also in Figure S-11: sample M-C (left column) and disulfide containing samples M-C-S10 (middle column) and M-C-S30 (right column). Samples were stirred in water for 3 h using the standard concentration of 0.1 mg/mL and additionally at concentrations of 0.2 mg/mL and 0.4 mg/mL. The supernatants obtained after centrifugation were then measured with UV-VIS spectroscopy. The individual samples were prepared from the same labeled stock solutions by dilution and measured on the same day. We found a pronounced decrease of dye release upon increasing the MSN concentration. This effect is strongest for the sample with the highest S-S concentration.

Figure S-17: zeta potential measurements

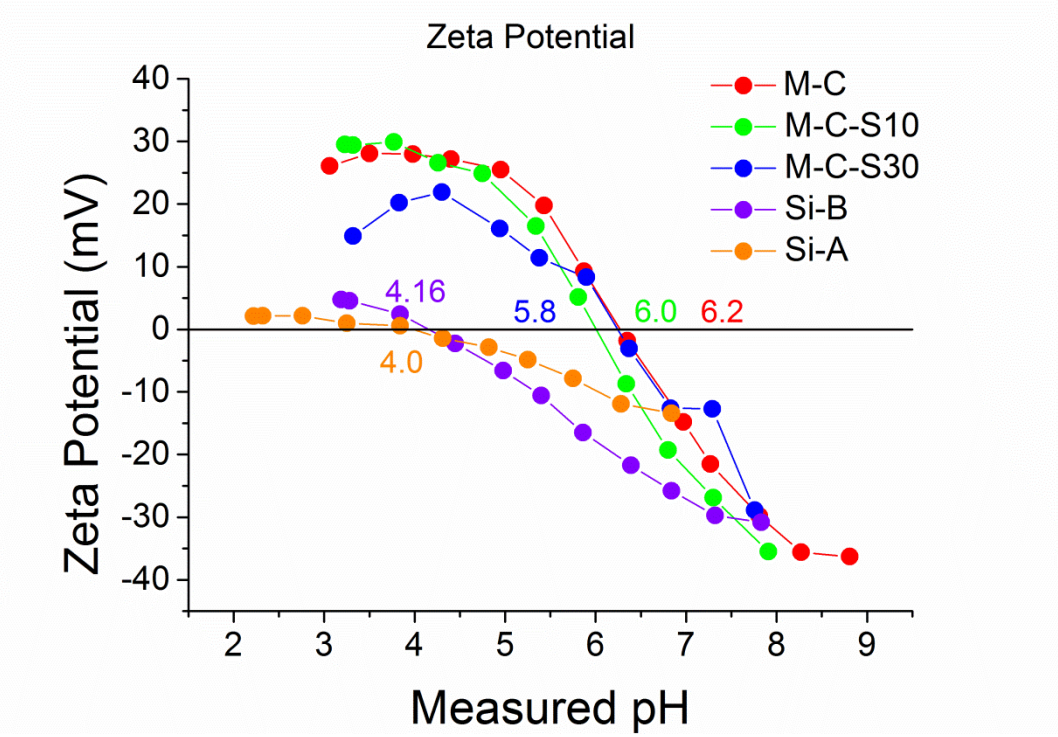

Figure S-17: Zeta potential measurements of purely siliceous samples Si-A and Si-B as well as co-condensed sample M-C and samples M-C-S10 and M-C-S30, co-condensed and additionally containing 10 and 30 mol% disulfide-bridged silanes in the particle, respectively.

We observe a clear distinction between purely siliceous and co-condensed samples when we measure the zeta potential. The non-functionalized samples show an isoelectric point (IEP) of around pH 4, with the sample made under acidic conditions having a small slope running close to zero over a broad range. This sample contains much fewer hydroxyl groups (also demonstrated in the NMR data) and thus is less affected by de-/protonation. We have reported before[29] that we can increase the IEP by implementing amino groups either by grafting or co-condensation, and accordingly for the co-condensed samples M-C, M-C-S10 and M-C-S30 we observe a higher IEP value of around pH 6 and observe much steeper zeta potential functions. Hence, these samples are more easily affected by protonation which might contribute to their hydrolytic degradability.

Figure S-18: Long-term degradation of the purely siliceous sample Si-B with varying concentrations

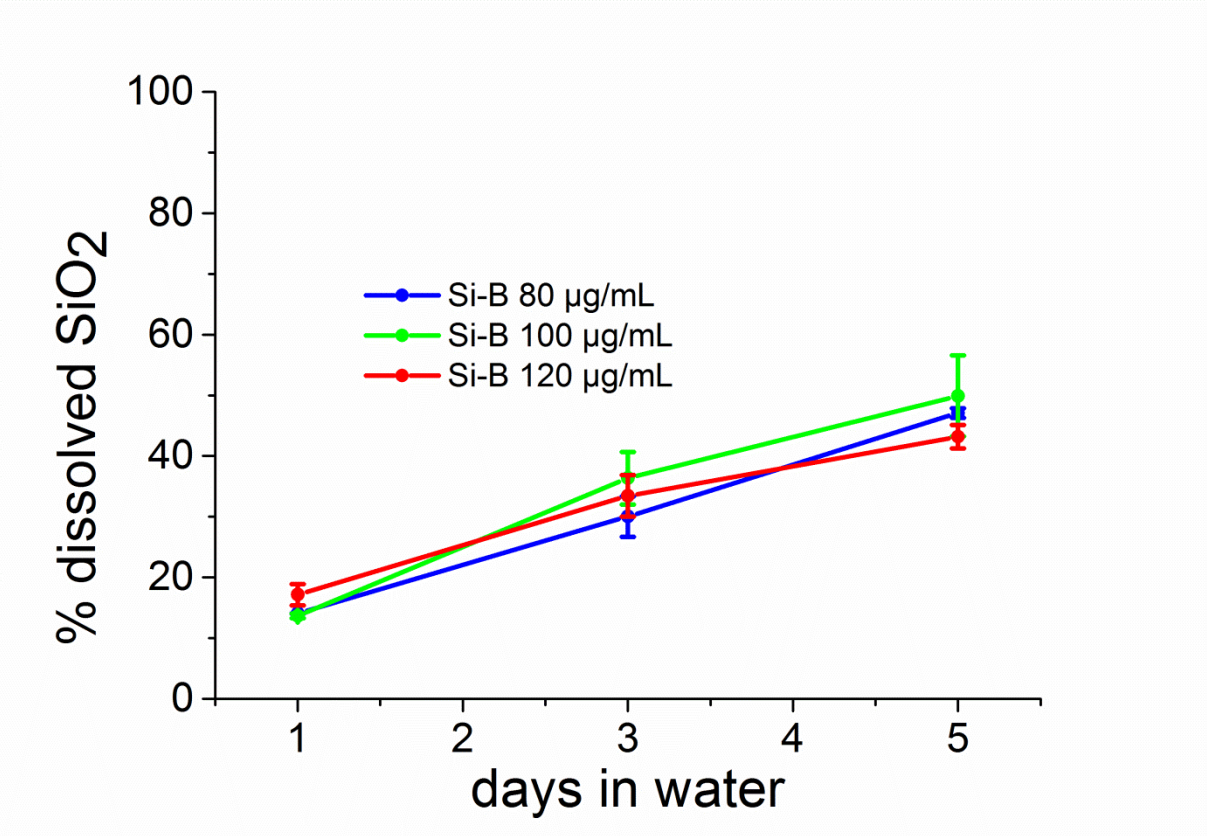

Figure S-18: The sensitivity of the dissolution behavior of the purely siliceous sample Si-B was studied at concentrations between 80 and 120 µg/mL. It shows a degradability (dissolution rate) that is nearly independent of small concentration variations, and furthermore documents the reproducibility of our measurements.

Table S-4: NMR compilations of chemical shifts and relative concentrations of silicon species in MSN samples

$^{29}Si\{^{1}H\}$ CP-MAS-NMR Rel. Conc (%)								
	Si-A		**Si-B**		**M-C**		**M-C-S30**	
	δ Si	%	δ Si	%	δ Si	%	δ Si	%
Q^4	-112	21.0	-111	16.0	-111	16.4	-110	15.0
Q^3	-102	75.0	-101	78.0	-101	64.0	-102	36.8
Q^2	- 92	4.0	- 92	6.0	- 92	2.35	- 90	1.6
T^3					- 67	12.8	- 67	37.3
T^2					- 58	0.45	- 60	9.2
^{29}Si DP-MAS NMR Rel. Conc (%)								
	Si-A		**Si-B**		**M-C**		**M-C-S30**	
	δ Si	%	δ Si	%	δ Si	%	δ Si	%
Q^4	-112	70.3	-111	56.6	-111	59.4	-111	47.2
Q^3	-103	29.7	-102	43.3	-102	33.8	-102	18.9
Q^2					- 93	0.9		
T^3					- 66	3.1	- 68	33.8
T^2					- 58	2.7		

Table S-4: Cross-polarized (CP) and directly-polarized (DP) ^{29}Si Solid State NMR results of selected samples showing the chemical shifts and the relative percentage of the integrated areas of the individual signals.

Figure S-19: Influence of protein adsorption on dissolution

In order to get a more realistic picture of the dissolution behavior under simulated biological conditions we tested the dissolution stability in water of three selected MSN samples after being exposed to Fetal Bovine Serum FBS, which contains many proteins that are encountered when samples are administered systemically. Our samples included the purely siliceous sample Si-B, and two samples where either (i) the inner pore or (ii) the outer shell is protected by (i) a phenyl residue (sample M-C-Ph; 1 % phenyltriethoxysilane core/1 % SH shell) or (ii) a peripheral PEG linker (sample M-C-PEG; 9% NH_2 core /1% PEG shell, the latter coupled via mecapto groups).

An amount of 1 mg sample each was stirred for 1 hour in FBS at 37°C, washed and then finally studied in aqueous solution as before (0.1 mg/mL, 37 °C). Aliquots from the time series were analyzed by ICP and the results are shown in **Figure S-19**. Sample Si-B shows a similar low dissolution behavior before and after being exposed to FBS. Similarly, the 1% co-condensed sample M-C-Ph is only dissolved to an extent of about 30 % after 3 days. Surprisingly, sample M-C-PEG (green curve) is much more stable after this treatment. Here, we measured only 38 % dissolved silica after 3 h, which increased to only 48 % after 3 days. This is in strong contrast to the near complete dissolution of this sample when it is not exposed to FBS (see also **Figure 2** and additional points included here, in **Figure S-19** after 3 d).

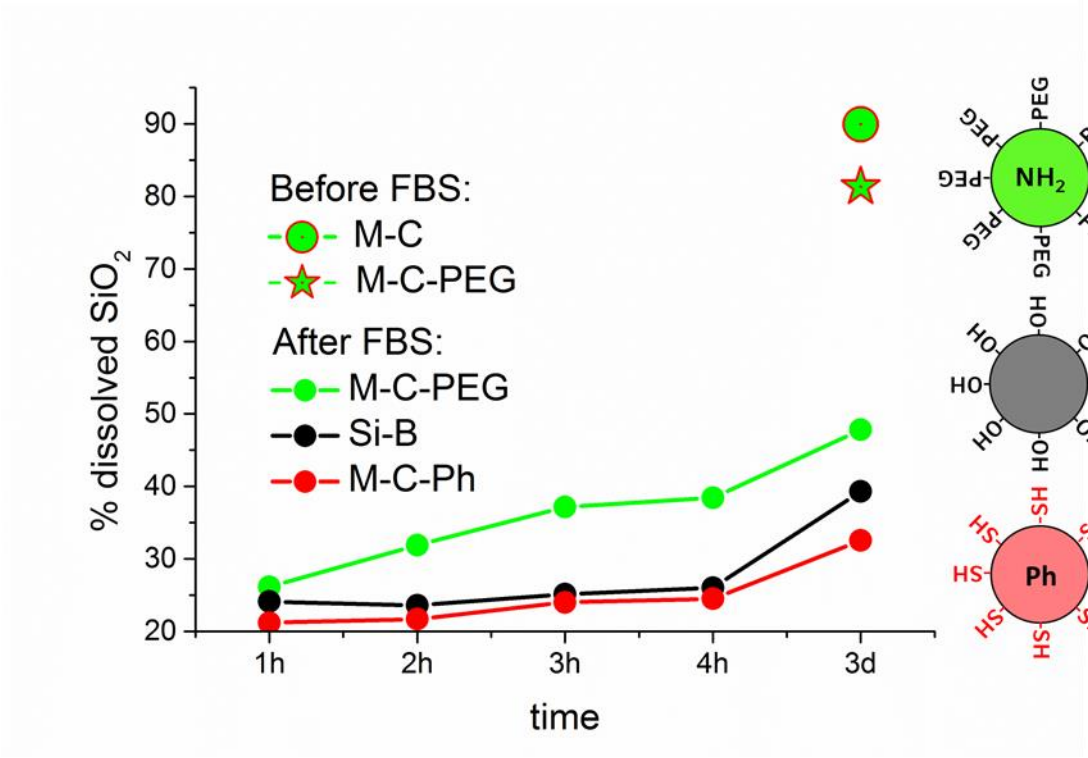

Figure S-19: ICP results for samples after pretreatment in FBS for 1 h at 37 °C. Dissolution was studied for washed samples under similar conditions as above (aqueous solution, 0.1 mg/mL, 37 °C). A plain silica sample Si-B is compared to two co-condensed samples: M-C-Ph (red) with 1 % phenyl groups in the core and 1 % SH in the shell, and M-C-PEG (green) with 9 mol% NH_2 in the core and 1 % SH in a shell that was coupled to PEG750. For comparison the latter sample is also shown after 3 d without being exposed to FBS (green dot and star, with and without PEG shell, respectively).

All of these samples, including the PEGylated sample M-C-PEG, have acquired a substantial protein layer from the FBS that is partially retained even after extensive washing, as seen in FTIR spectra of the remaining solid residues (see Figure **S-20**).

Figure S-20: FTIR spectra of samples M-C-Ph and M-C-PEG after exposure to FBS showing protein adsorption

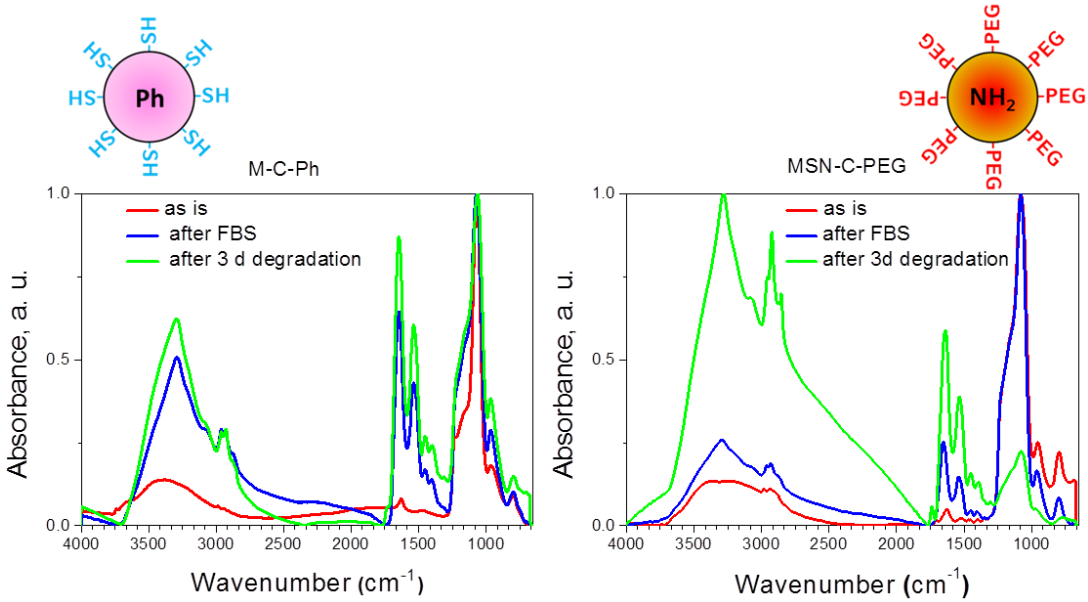

Figure S-20: FTIR spectra of samples M-C-Ph and M-C-PEG after exposure to a 10 % FBS solution. Samples were exposed to FBS for 1 h at 37°C under shaking and subsequently washed with water followed by centrifugation. Aliquots of 0.1 mg/mL were then stirred as usual at 37 °C and supernatants were retrieved each hour for 4 hours and a final sample was retrieved after 3 days. The solid cakes of samples directly retrieved after FBS exposure and after stirring in water for 3 days were then analyzed by FTIR spectroscopy and compared to the untreated sample, as shown above. The silica peak at 1080 cm^{-1} in sample M-C-PEG is strongly reduced after 3 days (green curve) in contrast to sample M-C-Ph, while the protein signatures are visible in all samples.